Advanced Steel Construction – Vol. 18 No. 3 (2022) 658–669
DOI:10.18057/IJASC.2022.18.3.3

ENERGY DISSIPATION OF STEEL-CONCRETE COMPOSITE BEAMS SUBJECTED TO VERTICAL CYCLIC LOADING

Jing Liu [1], Fei Lyu [2,*], Fa-Xing Ding [2,*] and Xue-Mei Liu [3]

[1] *School of Civil Engineering, Hunan City University, Yiyang, Hunan Province, 413000, P. R. China*
[2] *School of Civil Engineering, Central South University, Changsha, Hunan Province, 410075, P. R. China*
[3] *Department of Infrastructure Engineering, The University of Melbourne, Parkville, VIC 3010, Australia*
** (Corresponding author: E-mail: lyufei@csu.edu.cn; dinfaxin@csu.edu.cn)*

ABSTRACT

The finite element (FE) software ABAQUS was used to establish a 3D FE model and perform a pseudo-static analysis of steel–concrete composite beams. With the validated model, the influences of several key parameters, including shear connection degree, force ratio, and transverse reinforcement ratio, on seismic behavior were investigated and discussed. In addition, the working performance of studs was analyzed. The FE analysis results show that the steel girder is the main energy dissipation component of the composite beam, and the energy dissipation of the steel girder is more than 80% of the total energy. The next is longitudinal reinforcement, followed by a concrete slab, the minimum proportion is the studs. Results show that the energy dissipation ratio of studs is less than 1% under the condition of the parameters. However, an increase in shear connection is beneficial to improve the energy dissipation of steel girders and rebars. Shear connection, force ratio, and steel girder width–thickness ratio are the major factors that influence bearing capacity and seismic behavior. Transverse reinforcement, section form, and stud diameter are the secondary factors. Finally, a seismic design for composite beams was established.

ARTICLE HISTORY

Received: 2 June 2021
Revised: 14 December 2021
Accepted: 21 December 2021

KEYWORDS

Steel–concrete composite beam;
Shear connection degree;
Plastic energy consumption;
Hysteretic behavior

Copyright © 2022 by The Hong Kong Institute of Steel Construction. All rights reserved.

1. Introduction

Steel–concrete composite beams have been applied large-scale to civil structures, such as bridges and buildings, in recent years because of their high capacity, small section size, lightweight, and convenient construction. These benefits accrue from the combination of advantages of different constituent materials and the elimination of shortcomings of steel and concrete [1]. However, the composite steel beam–reinforced concrete (RC) slab behaviors are not customary to be considered in the design. The reason is partially because the composite beam have been mainly used in high-rise building applications at early stages so that the steel beam is designed relatively deep. The contribution of RC slab to the beam stiffness and strength is, therefore, insignificant [2]. Nevertheless, research works of understanding of steel beam-RC slab co-work mechanism promoted the application of composite beams on low-to-moderate height structures in recent years. In this case, the composite action between RC slab and steel girder may have a considerable influence on its hysteretic behaviors [3]. To date, most of the experimental and analytical study of composite beams focused on its static performance and fatigue life at which failure of the shank of the shear stud occurs [4-8]. The study on the seismic property of composite beams remains underdeveloped. Hence, to explore further the co-work mechanism of the composite beam under seismic load is of great importance to complement current design codes so that the steel beam-RC slab behaviors can be rationally considered in the aseismic design.

Recently, scholars from various countries have conducted extensive experiments to explore on the seismic property of steel–concrete composite beams. Reference [9-12] presented detailed experimental investigations of simply supported composite beams under vertical cyclic load (Fig. 1) and discussed the influences of several key parameters, such as the shear connection degree, width–thickness ratio, and transverse reinforcement ratio, of steel girders, on seismic behavior. This testing scheme is relatively rarely presented but meaningful for the following reasons: (1) In the aseismic design, a strong column–weak beam means that the plastic hinge appeared at the beam end for frame structure, which improved the ductility of the structure and prevented the collapse of buildings when subjected to severe shaking. Moreover, beams should have adequate shear and bending load capacity to develop plastic hinges under earthquake action. In general, the quasi-static test of the strong column-weak beam should be conducted, but the fabrication of specimens and experiments is costly and complicated. Thus, for simplicity, the experimental study of seismic performance of simply supported composite beams bearing the quasi-static cycle loading can be performed as a reasonable alternative. (2) The non-uniform settlement of buildings induced the bending moment and shear force that appeared at the beam end, which is highly similar when a vertical force is applied to the simply supported composite beam. (3) Low-frequency vertical cyclic loading is performed to study the hysteretic behavior in the node-negative moment region for the steel-concrete composite structure system. On the other hand, many theoretical models have been established and can be roughly categorized into two types [13].

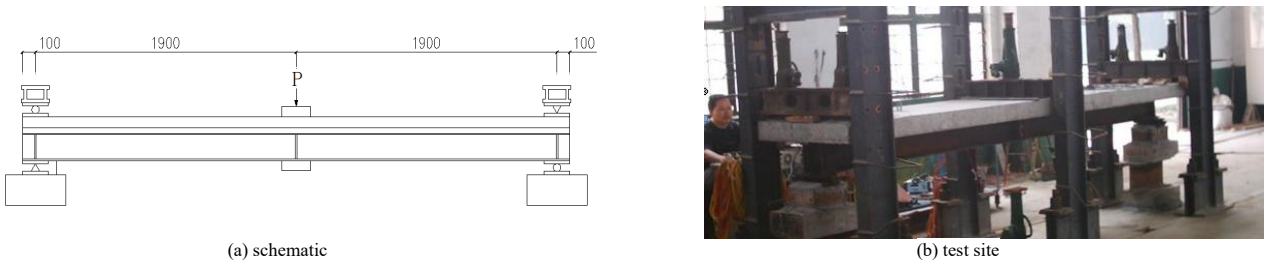

(a) schematic

(b) test site

Fig. 1 Experimental setup for vertical cyclic load

(1) Macro models: using line or frame elements and spring connectors to simulate the structural behaviors macroscopically. That is, the composite action between every structural member is implicitly reflected in the structural responses such as displacement and reactional force of nodes. These models usually make use of self-compiled and redeveloped programs to build the simplified descriptions of composite beams and commonly incorporate calibrated material constitutive models and load-slip models of connectors. For instance, Nie *et al*. [14] performed this process on composite beams under repeated and cyclic loadings. Based on the experimental research, the author established a restoring force model of steel–concrete composite beams by

considering the shear connection degree. A proposed fiber beam model was used to simulate the effects of an earthquake by Wang *et al*. [15] and Tao *et al*. [16], using MSC Marc or ABAQUS software. Ayoub and Filippou [1] proposed an inelastic beam element model for calculating steel–concrete beams partially connected under drab and cyclic loads. Zhao *et al*. [17] developed a high-efficiency macro-modelling program to analyze the nonlinear mechanical behavior of composite structural connections that consist of concrete-filled steel tubular (CFST) columns and steel-concrete composite beams [15].

(2) Micromodels: using continuum finite element (FE) modelling method, for example, solid or shell elements, to build the model contains complete geometric, boundary, and contact properties of the object structure. These models generally make use of universal FE software, such as ABAQUS and ANSYS. Research works employing this analytical technique. For instance, Nie *et al*. [18] investigated the seismic behavior of connections that were composed of steel CFST columns and steel–concrete composite beams. Then, 3D nonlinear FE models were proposed to research the mechanical character of three forms of connection via ANSYS. Bursi *et al*. [19] researched the seismic behavior of steel–concrete composite frames with a partial and full degree of shear connection and then suggested that shear connection degree should be sufficiently high to protect the shear connectors from damage. Vasdravellis *et al*. [20] evaluated the effect of partial composite action between steel girder and concrete slab of composite frames under seismic loading through ABAQUS.

At present, the research on the hysteretic performance of steel–concrete composite beams remains insufficient. Previous studies have failed to reflect stud energy dissipation capacity and its effect on structure energy dissipation distribution reasonably. In addition, the earthquake-resistant design of composite beams lacks a theoretical basis. Therefore, the present study aims to entirely research the seismic performance of steel–concrete composite beams and identify the working mechanism of studs. To this end, the vertical quasi-static finite analysis of simply supported composite beam is applied to simulate earthquake action in this study. The rationality of this test scheme on the study of seismic behaviors of composite beams has been illustrated before. Moreover, a previous experimental study [21] conducted by authors provides a solid verification of established FE models.

Based on the previous research of our team [22, 23], our current work has the following objectives. (1) A 3D solid model of steel beam–RC slab composite beams is established, and quasi-static analysis is conducted using ABAQUS software. The plastic damage constitutive model of concrete is adopted. The accuracy of the established model is fully verified against previous test results. (2) The effects of several parameters on the seismic property of composite beams are analyzed. The working performance of the stud of steel-concrete composite beams is investigated. The influences of the girder, longitudinal reinforcement, concrete slab, and stud on the components and integral energy dissipation of steel-concrete composite beams are determined. (3) To discuss the contribution of every structural component on resistance to seismic load from the point of view of energy dissipation. (4) To propose reasonable seismic structural measures for composite beams according to the FE analysis (FEA) results.

2. FEA

The author designed 11 I-shaped and 11 box steel beam–RC slab composite beams in the literature [12]. In the current work, a pseudo-static test of composite beams was conducted via FEA, and the validity is examined against the experimental results available in the literature [3, 12]. As mentioned above, a considerable number of analytical models were proposed by various researchers. However, most of the existing models are macro models that are essentially a design tool rather than an analytical tool because of their high simplicity. As such, the continuum element method was adopted for the steel beam and RC slab in this study to reproduce detailed experimental observation. Meanwhile, the dimension of stud in the composite beams is relatively small compared with the overall model scale so that rational simplicity can be exploited to save the computation cost. As a result, a hybrid modelling method that contains solid, shell, and liner elements were adopted in this study to perform the analytical study of pseudo-static test.

2.1. FE modelling

2.1.1. Material constitutive models

The FE software ABAQUS/Standard 6.14 [24] was used in this study for detailed FE modelling. The material constitutive relationship of the concrete and steel was adopted from Ding *et al.* [21, 23].

2.1.2. Mesh and element

FE models are established via the ABAQUS program [24]. The modelling method uses four-node shell elements (S4R) to model steel beams and a two-node linear beam element (B31) to model studs (Fig. 2(a)). In addition, concrete is modelled using C3D8R (Fig. 2(b)). The reinforcement bars are modelled by a two-node linear truss element (T3D2) (Fig. 2(c)).

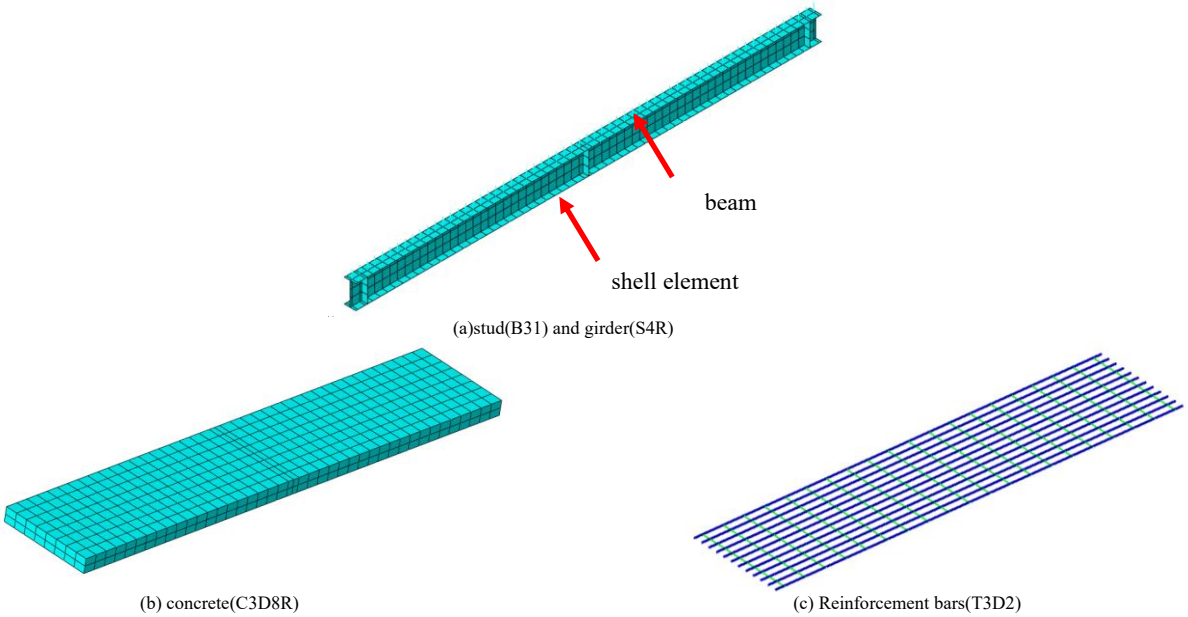

(a)stud(B31) and girder(S4R)

(b) concrete(C3D8R)

(c) Reinforcement bars(T3D2)

Fig. 2 Simplified FE models for steel-concrete composite beams

A structured meshing technique and static general step were adopted in this study. Fig. 3 shows simplified FE models for steel–concrete composite beams. The interaction between the upper surface of the steel girder and the bottom surface of the concrete slab is simulated by the optional contact surface model in ABAQUS, which is the most rational modelling approach and is widely applied in previous studies [25,26]. The use of spring element is an efficient way to enable interactions between shear studs and the concrete slab [27]. In this study, a more realistic approach that the stud elements were embedded in the concrete solid elements was adopted to simulate the composite actions. Detailed information about the mesh convergence and contact type is available in the literature [21,28]. The boundary of the steel–concrete composite beams was simply supported, similar to that in the FE model.

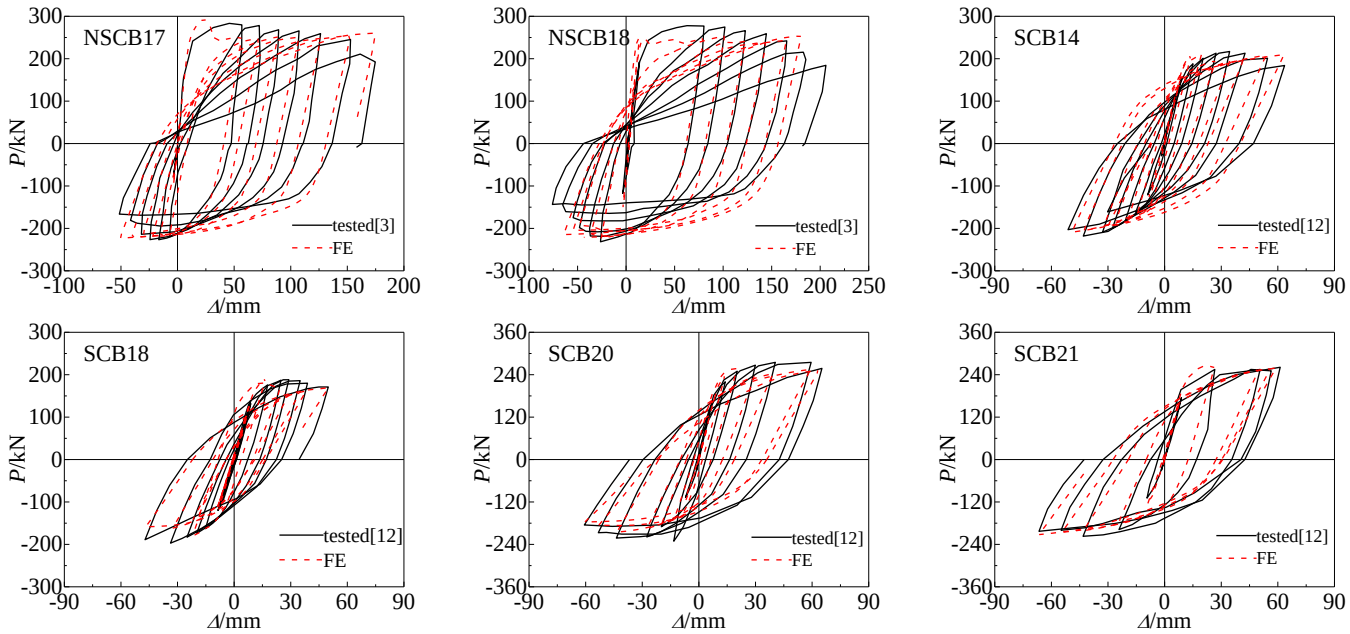

Fig. 3 Comparison between calculated and tested load-deformation hysteresis curve of steel-concrete composite beam

2.2. Model validation

2.2.1. Load–deformation curve

FE models were established to study the hysteretic performance of specimens using ABAQUS/Standard 6.10 [24]. The typical load–deflection hysteresis curves of the specimens that were obtained through FE analysis (FEA) compared with the experimental results are shown in Fig. 2, the test data were obtained from Nie *et al*. [3] and our team[12]. The load–deflection skeleton curve of steel–concrete composite beams is shown in Fig. 4, where Δ is the displacement in mid-span, and P is the vertical load. Loading displacement is considered positive or negative in the direction of loading is downward or upward, respectively.

Notably, the FE method provided an accurate experimental result. The FEA results of the ultimate bending capacity and flexural stiffness from the parametric analysis were compared with the tested ones (Fig. 5). The first method was used to calculate the FE modelling results, which are in good agreement with a maximum discrepancy of less than 10%.

2.2.2. Load–slip curve

The curves of slips at 1/4 span versus load are presented in Fig. 6. The figure shows that the FEA result agrees well with the experimental result.

2.2.3. Steel girder buckling

Fig. 7 compares the FEA and experiment results in terms of failure modes. The maximum buckling value of the steel web obtained by the FE method is 8.4 mm. The test result is 11.6 mm, thereby indicating that the FE method can simulate failure modes precisely.

Following the hysteresis curve, skeleton curve, load–slip curve, and failure mode, the FE method is reasonably performed for this study.

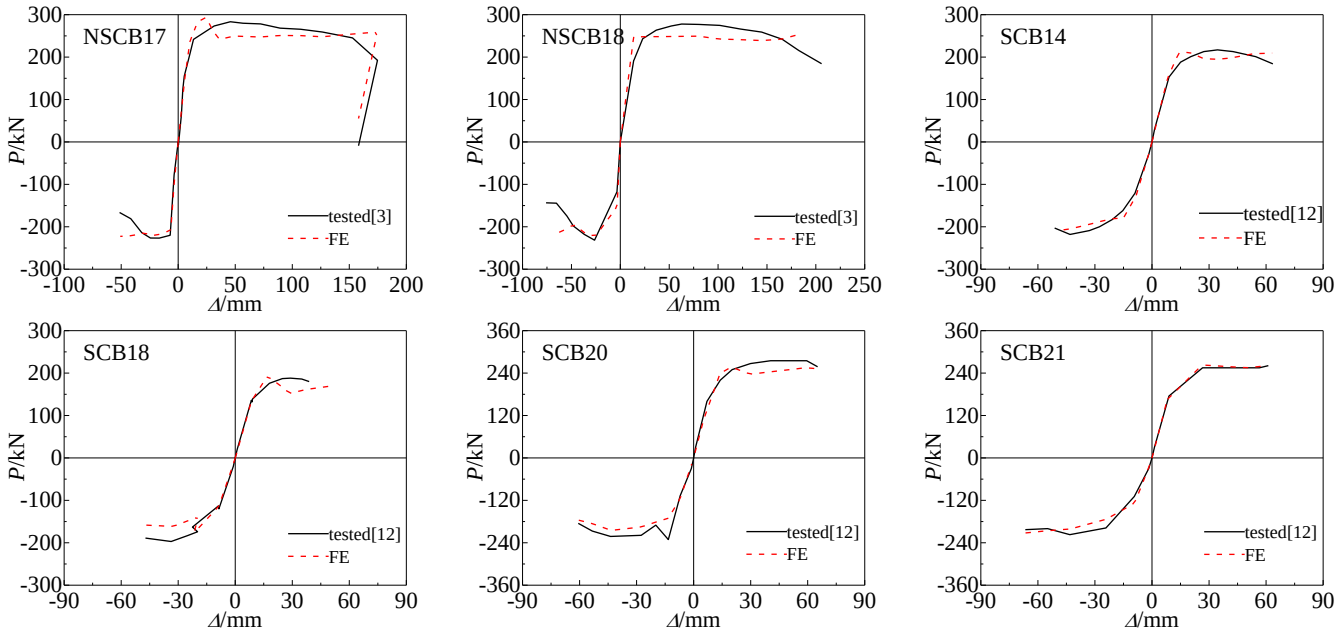

Fig. 4 Comparison between calculated and tested load-deformation skeleton curve of steel-concrete composite beam

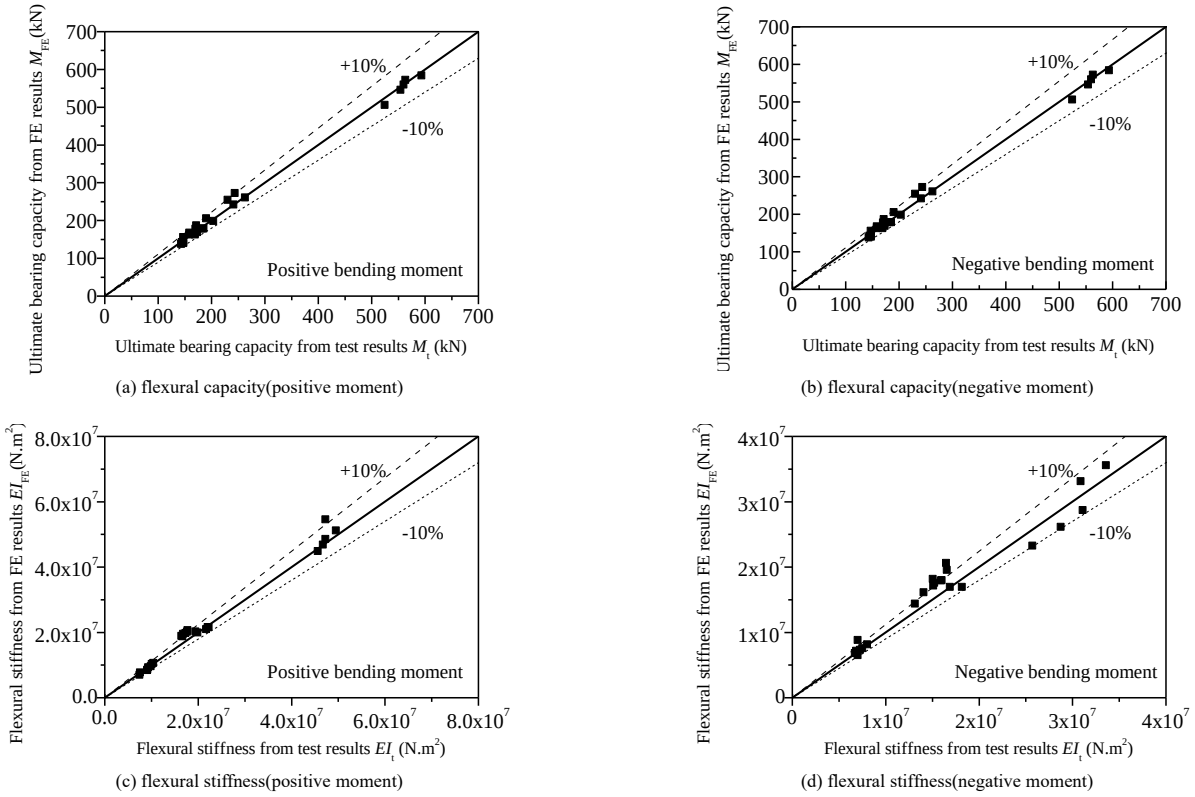

(a) flexural capacity(positive moment)

(b) flexural capacity(negative moment)

(c) flexural stiffness(positive moment)

(d) flexural stiffness(negative moment)

Fig. 5 Comparison between calculated and tested flexural capacity and stiffness of the composite beam

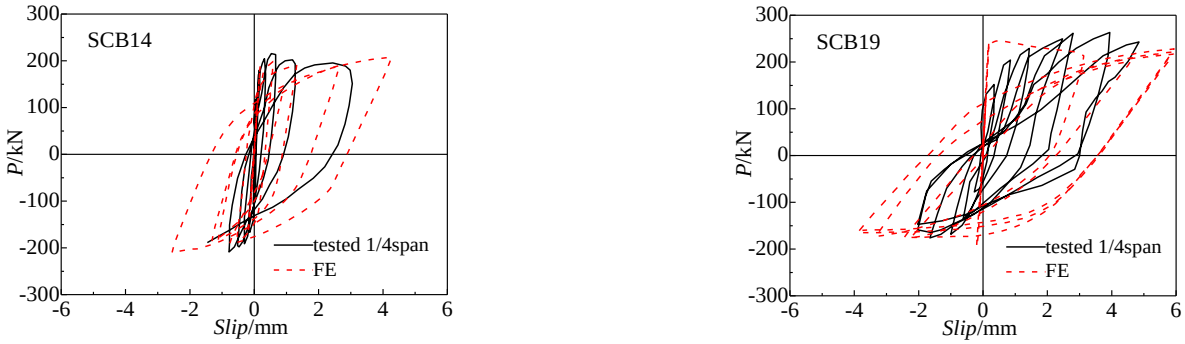

(a) SCB14

(b) SCB19

Fig. 6 Comparison between calculated and tested load-slip of composite steel-concrete beam

(a) test result

(b) FE result

Fig. 7 The failure modes comparison of FEA results and the experiment results

3. Parametric analysis

Six parameters that could affect the hysteretic behavior of composite beams, including transverse reinforcement ratio, shear connection degree, section form, force ratio, width–thickness ratio of the girder, and stud diameter, are investigated. A series of full-scale models was designed for parametric analysis using the nonlinear FE method. Table 1 demonstrates the detailed specimen parameters. Fig. 8 shows the cross-section of the girder. l is the length of the specimen; w_c and w_s are the widths of the concrete slab and the steel girder, respectively; h_c and h_s are the height of the concrete and steel girder, respectively; d is the diameter of the stud; ρ_t and ρ_l are the ratios of the transverse reinforcement and longitudinal reinforcements of the concrete slab, respectively; $f_{s,s}$ and f_u are the yield and ultimate strengths of the stud, respectively; f_{cu} is the cubic compressive strength of concrete; and $f_{s,b}$ is the yield strength of the girder.

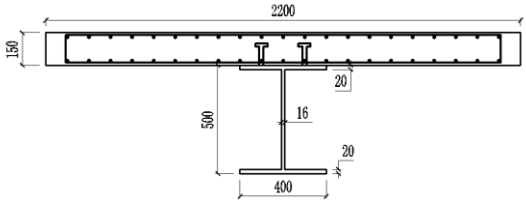

Fig. 8 Cross-section details of the girder

Table 1
Geometric properties and characteristics of composite beams

l/m	w_c/m	h_c/m	w_s/m	h_s/m	d/mm	ρ_t/%	ρ_l/%	$f_{s,s}$/MPa	f_u/MPa	f_{cu}/ Mpa	$f_{s,b}$/ MPa
12	2.2	0.15	0.4	0.5	19	0.19	2.56	350	455	40	345

3.1. Influence of shear connection degree

Existing research reveals that the degree of shear connection exerts a remarkable effect on the hysteretic behavior of composite beams [11,29]. The calculation method for shear connection degree in the sagging moment or hogging moment region is defined. In this article, the shear connection degree in the positive moment was applied to distinguish from different beams.

The shear connection degree in the sagging moment region η^+ is presented as follows (China Architecture and Building Press 2017):

$$\eta^+ = n / n_f \tag{1}$$

Formula (1) parameters are defined in [12].

$$V_u = (0.2d^{0.5} - 10) f_{cu}^{\,0.8-0.15\ln(d-10)} (0.002 f_y + 0.24) \tag{2}$$

A_{sd} is the cross-section area of the stud, f_c is the concrete compressive strength, and E_c is the concrete Young's modulus.

Figs. 9–10 and Table 2 compare the effect of shear connection degree on the hysteresis property of composite beams. The flexural stiffness could be attained as the secant stiffness at 0.4 times the ultimate load using the envelop curve. In Fig. 10, the slip was measured at the end of the beams, the lateral deformation means the displacement difference between stud top and stud bottom, and the shear force or moment is at the section of the stud bottom. The following points were observed.

(1) The plastic energy dissipation of the steel girder, reinforcement, and the entire model increases with the connection degree. When the connection degree increased from 0.5 to 1.0, the plastic energy dissipation values increased from 1209.0 kJ to 1446.3 kJ, which was an increase of 19.6%. This increment was primarily caused by an increase in the plastic energy consumption of the steel girder and bar. The single stud plastic energy dissipation value decreased from 64.2 kJ to 32.6 kJ, which was a decrease of 49.2%. The energy consumption of a single stud decreases as the stud number increases.

(2) For the positive moment region, the higher the shear connection degree is, the larger the flexural capacity and stiffness will be. Furthermore, composite beams illustrate good interaction behavior when η^+ is high, which can reduce the deflection of the composite beams under vertical loading and guarantee carrying capacity. However, this phenomenon is inevident when the connection degree is more than 1. The capacity of scb6(η^+=2.0) is 26.0% and 10.0% larger than those of scb2(η^+=0.5) and scb4(η^+=1.0), respectively. The stiffness of scb6(η^+=2.0) is 29.0% and 12.2% larger than those of scb2(η^+=0.5) and scb4(η^+=1.0), respectively.

For the negative moment region, the flexural capacity and stiffness difference is less than 1.1% and 1.0%, respectively, due to the shear connection degree(η-) being greater than 1 even for scb1.

(3) The slip peak value of scb2(η^+=0.5) is 32.3% and 168.5% larger than those of scb4(η^+=1.0) and scb6(η^+=2.0), respectively. The shearing force peak value of scb2(η^+=0.5) is 94.2% and 122.8% larger than those of scb4(η^+=1.0) and scb6(η^+=2.0), respectively. The moment peak value of scb2(η^+=0.5) is 71.1% and 106.7% larger than those of scb4(η^+=1.0) and scb6(η^+=2.0), respectively. These results indicate that the single stud force becomes weak with an increase in shear connection degree.

(4) According to Figs. 9(b) and 9(c), a sagging degree of shear connection should range from 1.0 to 1.3. The stud spacing in the hogging moment region should not be larger than that in the sagging moment region. The specimens exhibit good seismic properties.

Table 2
Influence of shear degree on plastic energy dissipation values

No.	η^+	space/mm	d/mm	plastic energy dissipation (kJ)					energy dissipation proportion of stud (%)	energy dissipation of each stud (J)
				Concrete slab	steel girder	reinforcement	stud	total		
scb1	0.25	800	19	40.0	1056.0	109.0	4.0	1209.0	0.33	133.3
scb2	0.5	400	19	45.0	1165.7	123.8	3.9	1338.4	0.29	64.2
scb3	0.67	300	19	47.7	1212.2	125.3	4.3	1389.5	0.31	53.9
scb4	1	200	19	40.5	1274.7	127.3	3.9	1446.3	0.27	32.6
scb5	1.3	150	19	45.7	1285.5	136.6	5.6	1473.5	0.38	28.1
scb6	2.0	100	19	43.8	1331.5	131.3	6.2	1512.8	0.41	26.0

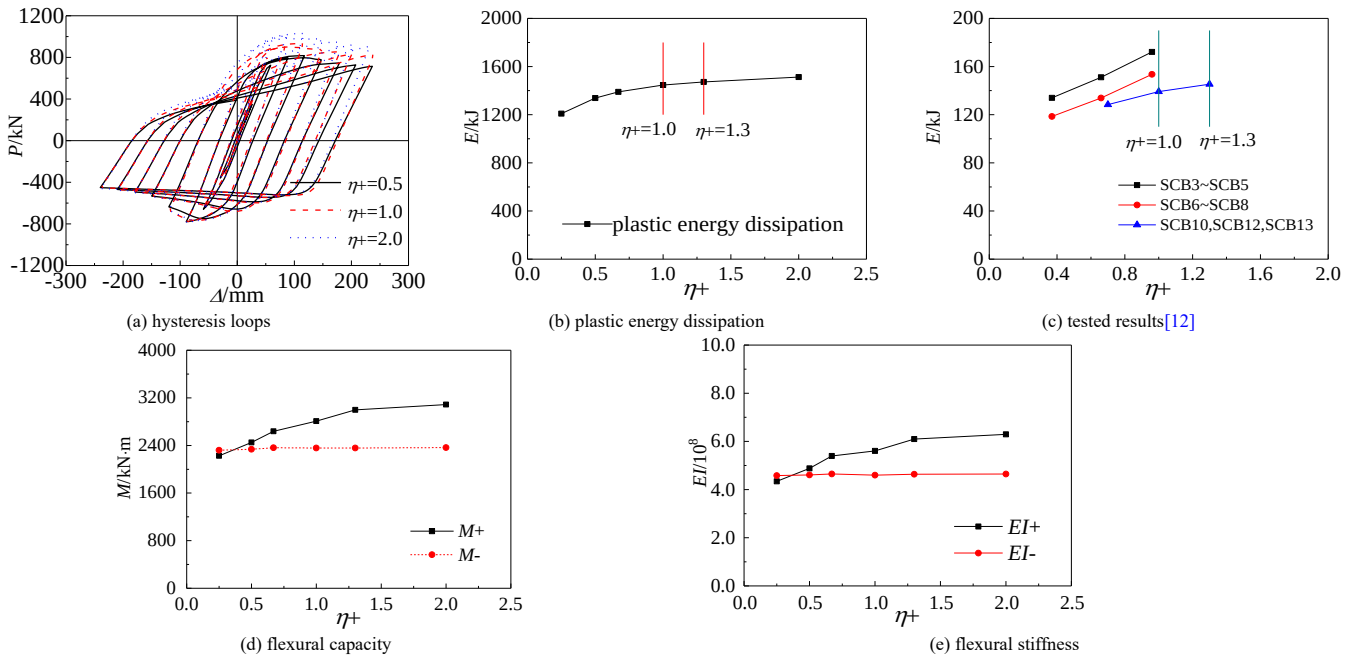

(a) hysteresis loops (b) plastic energy dissipation (c) tested results[12]

(d) flexural capacity (e) flexural stiffness

Fig. 9 Influence of shear connection on the hysteresis performance of steel-concrete composite beams

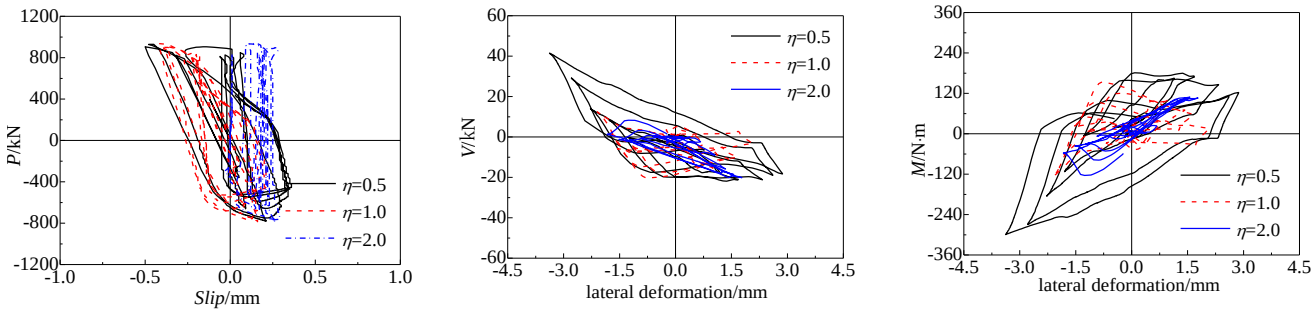

(a) loading-deformation (b) shear force of stud end-lateral deformation (c) moment of stud end-lateral deformation

Fig. 10 Influence of shear degree on the hysteresis performance of interface slip and stud mechanical performance of steel-concrete composite beams

3.2. Influence of force ratio

Force ratio considerably influences the plastic energy dissipation of steel–concrete composite beams. The force ratio can be determined by:

$$R = f_{s,l}A_{s,l} / f_{s,b}A_{s,b} \quad (3)$$

where $A_{s,l}$ and $A_{s,b}$ are the areas of the rebar and steel girder, respectively; and $f_{s,l}$ is the yield strength of the longitudinal rebar. Table 3 and Fig. 11 compare the influences of force ratio on the hysteresis performance of steel–concrete composite beams.

(1) The greater the force ratio is, the greater the reinforcement ratio will be. The greater the increase in rebar and composite beam energy dissipation is, the less the energy dissipation of the slab will be. The energy dissipation of studs is unaffected. Force ratio exerts a considerable impact on energy dissipation. That is, the energy dissipating capacity generally increases with the force ratio. When the force ratio increased from 0.07 to 0.64, the plastic energy dissipation value increased from 1282 kJ to 1615 kJ, which was an increase of 26.0%.

(2) The larger the force ratio is, the larger the negative bending capacity and flexural stiffness will be, and the positive bending capacity and flexural stiffness slightly increase. More longitudinal reinforcement that can bear force will exist because the force ratio is high. The negative bending capacity value of scb11(R=0.68) is 24.9% and 9.9% larger than those of scb7(R=0.07) and scb4(R=0.36), respectively. The negative flexural stiffness value of scb11(R=0.68) is 40.7% and 13.5% larger than those of scb7(R=0.07) and scb4(R=0.36), respectively.

Table 3
Influence of force ratio on plastic energy dissipation values

No.	η^+	space/mm	d/mm	R	plastic energy dissipation (kJ)					energy dissipation proportion of stud (%)	energy dissipation of each stud (J)
					concrete slab	steel girder	reinforcement	stud	total		
scb7	1.0	200	19	0.07	68.8	1129.8	74.6	4.6	1277.7	0.36	37.9
scb8	1.0	200	19	0.14	56.1	1167.1	102.0	4.1	1329.3	0.31	33.8
scb9	1.0	200	19	0.24	46.1	1231.9	110.6	4.0	1392.6	0.29	33.3
Scb4	1.0	200	19	0.36	40.5	1274.7	127.3	3.9	1446.3	0.27	32.6
scb10	1.0	200	19	0.51	35.8	1309.1	144.9	3.6	1493.4	0.24	29.6
scb11	1.0	200	19	0.68	36.1	1343.2	156.8	4.2	1540.3	0.27	34.9

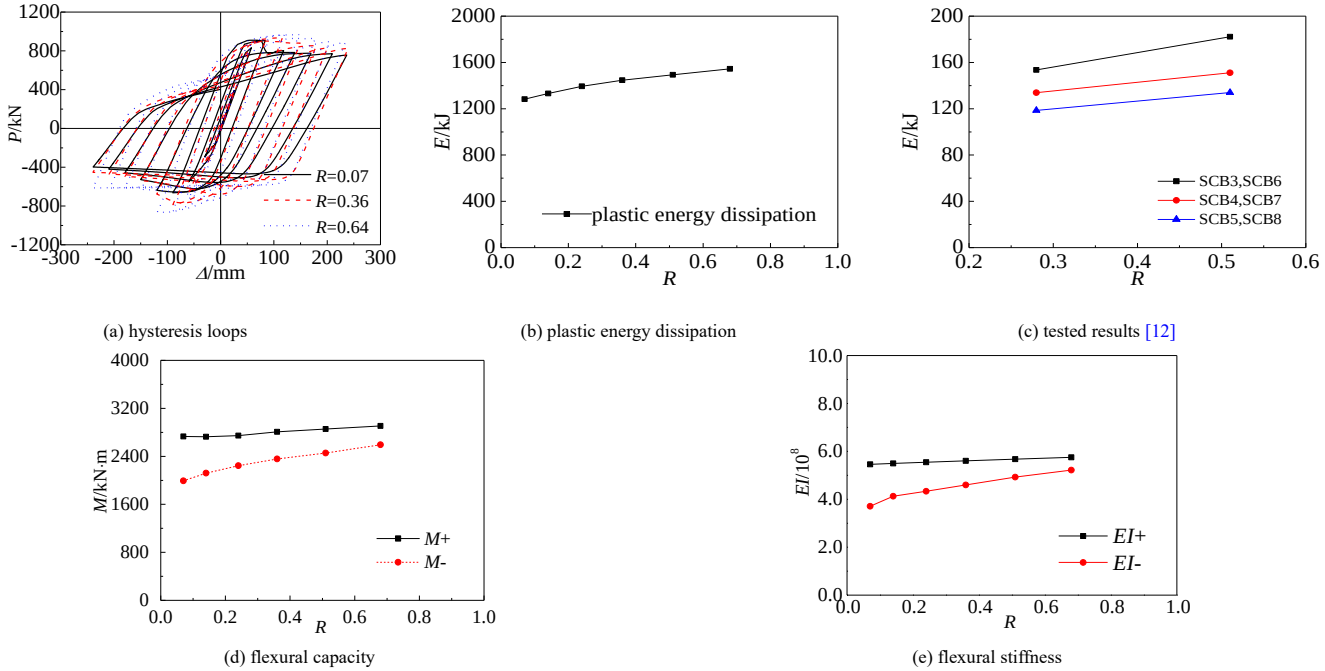

(a) hysteresis loops (b) plastic energy dissipation (c) tested results [12]

(d) flexural capacity (e) flexural stiffness

Fig. 11 Influence of force ratio on the hysteresis performance of steel-concrete composite beams

3.3. Influence of the width–thickness ratio of girders

Tables 4–5 and Figs. 12–13 compare the influences of the width–thickness ratio of a girder on the hysteresis property of specimens. R_w denotes the width–thickness ratio of the web. R_f indicates the width–thickness ratio of the flange. The following observations were noted.

(1) The width–thickness ratio exerts a considerable impact on plastic energy dissipation, which decreases with an increase in the width–thickness ratio. The plastic energy dissipation of scb15(R_w=19.2) is 17.8% and 48.4% larger than those of scb4(R_w=28.8) and scb12(R_w=57.5), respectively. The plastic energy dissipation of scb17(R_f=6.4) is 44.8% and 114.0% larger than those of scb4(R_f=9.6) and scb16(R_f=19.2), respectively. The energy dissipation of studs is only slightly affected by the width–thickness ratio.

(2) Bending capacity is decreased with an increase in the width–thickness ratio. The flexural capacity of scb15(R_w=19.2) is 13.8% and 34.7% larger than those of scb4(R_w=28.8) and scb12(R_w=57.5), respectively. The flexural capacity of scb17(R_f=6.4) is 27.9% and 90.6% larger than those of scb4 (R_f=9.6) and scb16(R_f=19.2), respectively.

Flexural stiffness is decreased with an increase in the width–thickness ratio. The flexural stiffness of scb15(R_w=19.2) is 7.1% and 17.0% larger than those of scb4(R_w=28.8) and scb12(R_w=57.5), respectively. The flexural stiffness of scb17(R_f=6.4) is 24.8% and 67.9% larger than those of scb4 (R_f=9.6) and scb16(R_f=19.2), respectively.

Table 4
Influence of width-thickness ratio of the web on plastic energy dissipation values

No.	η^+	space/mm	d/mm	R_w	plastic energy dissipation (kJ)					energy dissipation proportion of stud (%)	energy dissipation of each stud (J)
					concrete slab	steel girder	reinforcement	stud	total		
scb12	1.0	240	19	57.5	29.7	1015.3	100.1	3.3	1148.4	0.29	27.6
scb13	1.0	220	19	38.3	38.9	1224.5	118.4	5.8	1387.5	0.42	48.2
scb4	1.0	200	19	28.8	40.5	1274.7	127.3	3.9	1446.3	0.27	32.6
scb14	1.0	185	19	23.0	49.9	1392.7	147.1	5.2	1594.9	0.32	43.0
scb15	1.0	175	19	19.2	55.7	1464.9	178.2	5.6	1704.5	0.33	46.9

Explanation: t_f=20mm, the t_b is from 8mm to 24mm, R_w is from 55.7 to 19.2.

Table 5
Influence of width-thickness ratio of the flange on plastic energy dissipation values

No.	η^+	space/mm	d/mm	R_f	plastic energy dissipation (kJ)					energy dissipation proportion of stud (%)	energy dissipation of each stud (J)
					concrete slab	steel girder	reinforcement	stud	total		
scb16	1.0	300	19	19.2	28.9	862.6	83.8	4.2	979.6	0.43	35.4
scb17	1.0	240	19	12.8	37.6	1096.3	111.5	5.6	1251.0	0.45	46.6
scb4	1.0	200	19	9.6	40.5	1274.7	127.3	3.9	1446.3	0.27	32.6
scb18	1.0	170	19	7.7	47.9	1556.4	141.7	4.3	1750.3	0.25	35.9
scb19	1.0	160	19	6.4	55.1	1872.0	161.9	4.8	2093.9	0.23	40.0

Explanation: t_b =16mm, the t_f is from 10mm to 30mm, R_w is from 19.2 to 6.4.

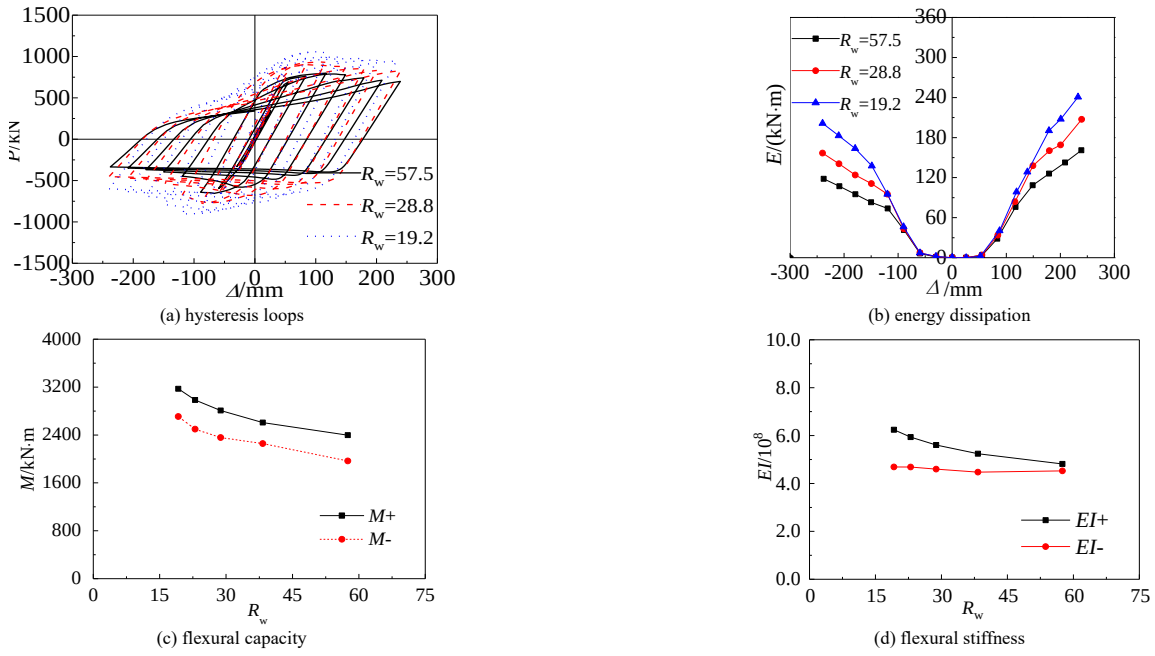

Fig. 12 Influence of width-thickness ratio of the web on the hysteresis performance of steel-concrete composite beams

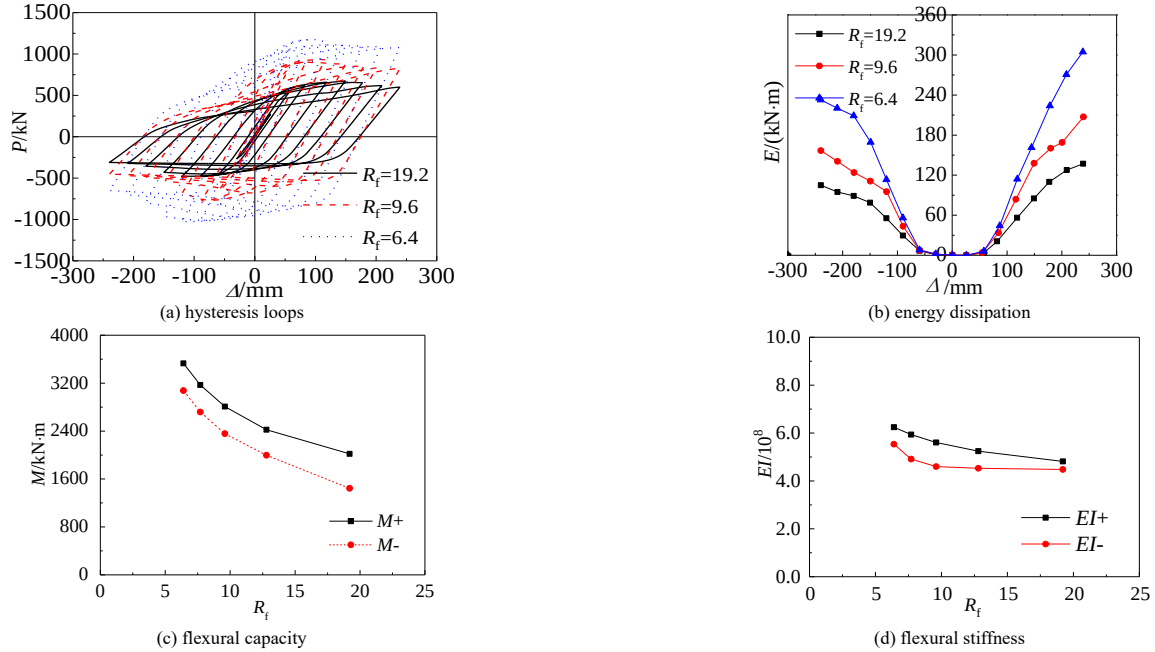

(a) hysteresis loops (b) energy dissipation (c) flexural capacity (d) flexural stiffness

Fig. 13 Influence of width-thickness ratio of the flange on the hysteresis performance of steel-concrete composite beams

Tables 6–7 compare the thickness of the steel girder and the specification requirement. Fig. 14 illustrates the effect of the width–thickness ratio on the capacity of steel–concrete composite beams. The following observations are made.

(1) In standard [30], when an I beam works under bending, $R_w=h_s/t_w \leq 65(235/f_{s,b})1/2$, $R_f=b/t_f \leq 9(235/f_{s,b})1/2$, b is the width of the web side, and $b=(w_b-t_w)/2$.

(2) The value of the width–thickness ratio is 57.5–19.2. Therefore, the specimen meets the requirements of the specification, except for t_w=8. The variation trend of the carrying capacity under the sagging moment of the FEA results is close to that of the standard results. However, when the thickness ratio of the web plate under the negative load changes from 38.3 to 57.5, the bearing capacity under the negative moment of the FEA results decreases faster than those of the standard results.

The value of the width–thickness ratio is 19.2–6.4. Hence, the specimen failed to meet the requirements of the specification, except for R_f=6.4. The variation trend of the bearing capacity under the positive moment of the FEA results is close to that of the standard results. In addition, when the thickness ratio of the web plate under the negative load changes from 12.8 to 19.2, the bearing capacity under the negative moment of the FEA results decreases faster than those of the standard results.

(3) The preceding analysis results show that the limit value of the width–thickness ratio can be relaxed, thereby limiting the values of the width–thickness ratio of the flange and the web to 15 and 45, respectively.

Table 6
The thickness of steel girder web compare with specification requirements

No.	t_w(mm)	t_f (mm)	R_w	65(235/$f_{s,b}$)1/2	meets requirements?
1	8	20	57.5	53.6	No
2	12	20	38.3	53.6	Yes
3	16	20	28.8	53.6	Yes
4	20	20	23.0	53.6	Yes
5	24	20	19.2	53.6	Yes

Table 7
The thickness of steel girder flange compare with specification requirements

No.	t_w (mm)	t_f (mm)	R_f	9(235/$f_{s,b}$)1/2	meets requirements?
1	16	10	19.2	7.4	No
2	16	15	12.8	7.4	No
3	16	20	9.6	7.4	No
4	16	25	7.7	7.4	No
5	16	30	6.4	7.4	Yes

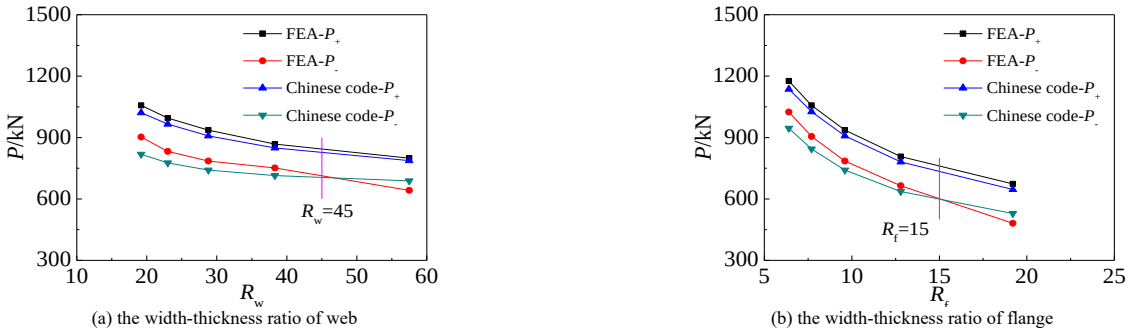

(a) the width-thickness ratio of web (b) the width-thickness ratio of flange

Fig. 14 Influence of width-thickness ratio on the capacity of steel-concrete composite beams

3.4. Influence of the transverse reinforcement ratio

Table 8 and Fig. 15 compare the influences of the transverse reinforcement ratio on the hysteresis property of specimens, and the findings are presented as follows:

(1) Plastic energy dissipation is slightly increased with the transverse reinforcement ratio. The plastic energy dissipation of scb3 (ρ_t=1.03) is 1.1% and 0.9% larger than those of scb24(ρ_t=0.19%) and scb21(ρ_t=0.52%), respectively. The energy dissipation of studs was less than 1% of the total energy.

(2) Bending capacity and flexural stiffness is slightly increased with an increment in the transverse reinforcement ratio, and the transverse stirrup ensures that the concrete slab and steel girder collaborate efficiently.

The capacity in the positive and negative moment regions of scb23(ρ_t=1.03) is 1.9% and 2.9% larger than those of scb4(ρ_t=0.19%), respectively. The stiffness in the positive and negative moment regions of scb23(ρ_t=1.03) is 0.1% and 0.2% larger than those of scb4(ρ_t=0.19%), respectively.

Table 8
Influence of transverse reinforcement on plastic energy dissipation values

No.	η^+	space/mm	d/mm	ρ_t /%	plastic energy dissipation (kJ)					energy dissipation proportion of stud (%)	energy dissipation of each stud (J)
					concrete slab	steel girder	reinforcement	stud	total		
scb4	1.0	200	19	0.19	40.5	1274.7	127.3	3.9	1446.3	0.27	32.6
scb20	1.0	200	19	0.33	38.2	1297.2	125.7	4.1	1465.2	0.28	34.3
scb21	1.0	200	19	0.52	38.5	1291.1	127.6	4.3	1461.5	0.29	35.9
scb22	1.0	200	19	0.75	35.8	1304.4	125.4	4.3	1469.9	0.29	36.1
scb23	1.0	200	19	1.03	34.2	1324.2	122.6	4.3	1485.2	0.29	35.5

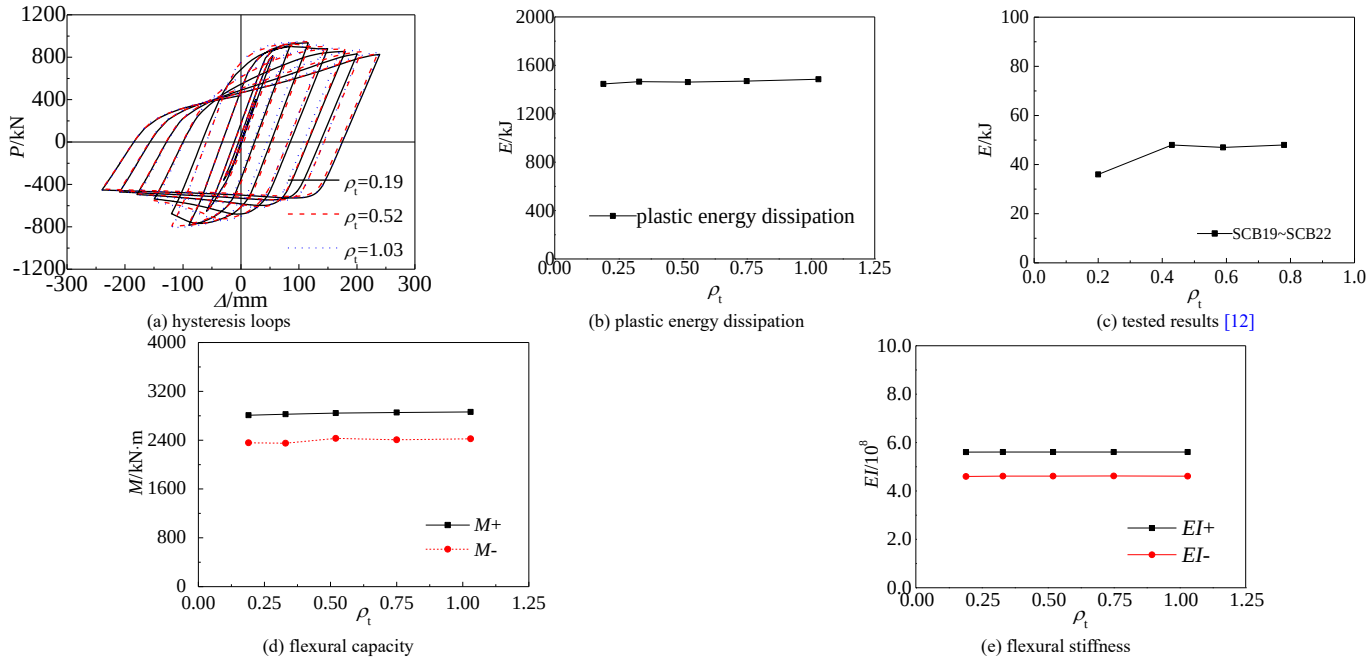

(a) hysteresis loops (b) plastic energy dissipation (c) tested results [12]

(d) flexural capacity (e) flexural stiffness

Fig. 15 Influence of transverse reinforcement ratio on the hysteresis performance of steel-concrete composite beams

The transverse stress measuring points were set from four typical positions in the heavily loaded region from 1/4 to 1/2 spans. Fig. 16 illustrates the arrangement of the transverse stress measuring points. Fig. 17 shows the influence of the transverse reinforcement ratio on concrete slab stress (normal stress) in the mid-span region under the positive bending moment. The following observations were made.

(1) Fig. 17(a) shows the transverse stress–displacement curve, where transverse stress reaches the maximum value when center deflection displacement reaches approximately 140 mm. However, transverse stress decreases with an increase in the transverse ratio, and the slab can barely exhibit longitudinal cracks, which agrees with the test result [12].

(2) Fig. 17(b) shows the effect of the transverse reinforcement ratio on the maximum concrete transverse stress at different locations. When the transverse reinforcement ratio is 0%–0.5%, stress decreases rapidly. However, when the transverse reinforcement ratio exceeds 1.0%, stress is reduced slowly. Therefore, the transverse reinforcement ratio is suggested to range from 0.5% to 1.0%.

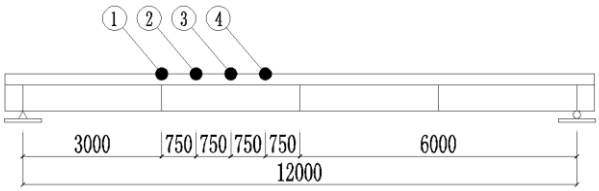

Fig. 16 The arrangement of the transverse stress measuring points

(a) time-history curve of slab stress-displacement

(b) curve of slab stress- transverse reinforcement ratio

Fig. 17 Influence of transverse reinforcement ratio on the stress of concrete slab

3.5. Influence of section form

Table 9 and Fig. 18 compare the influences of section form on the hysteresis property of specimens, and the findings are presented as follows:

(1) The I beam has a slightly larger plastic energy dissipation capacity than the box beam. At an equivalent limit deflection, the dissipation capacity of the I beam is 3.6% larger than that of the box beam. The energy dissipation of studs is less than 1% of the total energy.

(2) Compared with the box beam, the I beam has a minor fuller hysteretic curve. Moreover, the I beam has a slightly higher bending bearing capacity than the box-shaped ones. The bearing capacity in the sagging and hogging moments of the scb4 (I beam) specimen is 1.8% and 6.5% larger than that of the scb24 (box beam) specimen. The flexural stiffness difference between the I beam and the box beam is quite modest.

The single web of the I-shaped steel girder is twice as thick as that of the box-shaped girder. Therefore, when the two types of composite beams bear a negative limit load, the maximum transverse deformation of the I-shaped and box-shaped beams is 6.53 and 0.52 mm, respectively. This web of box-beam is half as thick as the web of the I beam because the box girder have two webs. Relatively speaking, the web of the bot-girder was weak, so the maximum transverse deformation is larger.

Table 9
Influence of section form on plastic energy dissipation values

No.	η^+	space/mm	*d*/mm	section form	plastic energy dissipation (kJ)					energy dissipation proportion of stud (%)	energy dissipation of each stud (J)
					concrete slab	steel girder	reinforcement	stud	total		
scb4	1.0	200	19	I beam	40.5	1274.7	127.3	3.9	1446.3	0.3	32.6
scb24	1.0	200	19	Box beam	36.5	1245.4	108.8	5.0	1395.7	0.4	41.8

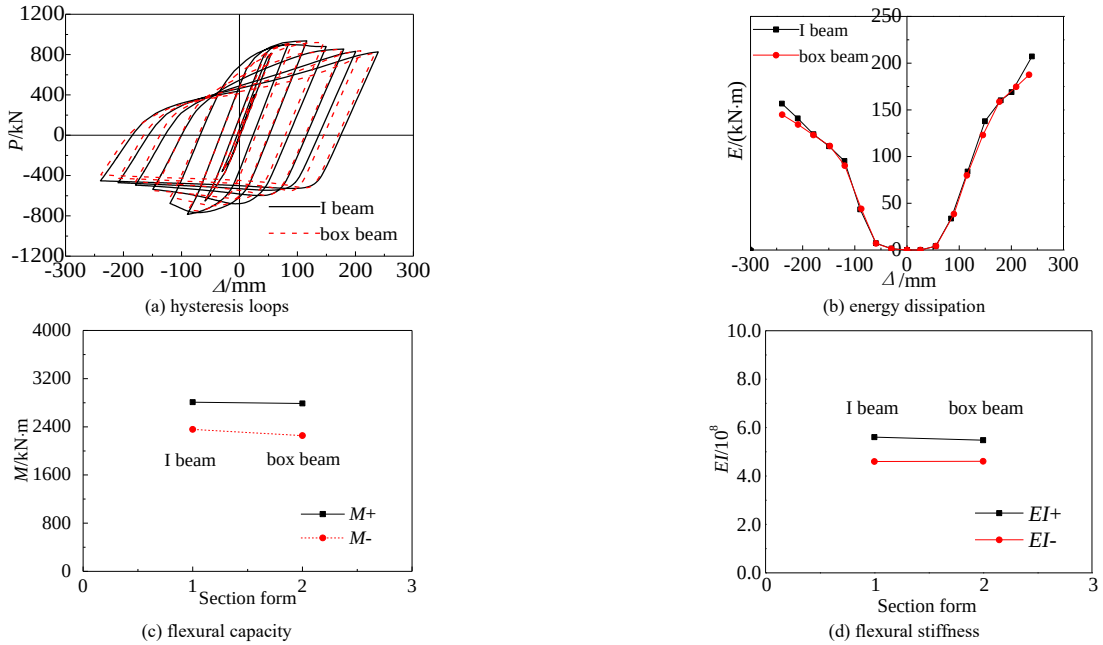

(a) hysteresis loops

(b) energy dissipation

(c) flexural capacity

(d) flexural stiffness

Fig. 18 Influence of section form on the hysteresis performance of steel-concrete composite beams

3.6. Influence of stud diameter

In structural or bridge engineering, excessive studs increase the obstruction in pouring concrete [31]. Table 10 and Fig. 19 compare the influences of stud diameter on the hysteresis property of the specimen. Researching seismic behavior under different stud diameters but the same shear connection degree is necessary for construction convenience.

(1) Stud diameter exerts an insignificant impact on plastic energy dissipation, with the largest difference between several samples being 2.6%. The plastic energy dissipation of each stud increases with stud diameter. The energy dissipation value of scb28(*d*=33 mm) is 274.5% and 141.3% larger than those of scb25(*d*=13 mm) and scb4(*d*=19 mm).

(2) Stud diameter influences the hysteresis curve of specimens minimally. The comparison of specimens illustrates that stud diameter has minimal effect on bearing capacity at the sagging or hogging moment region with the largest difference of at less than 0.6% and 1.0%, respectively. Moreover, the flexural stiffness difference at the positive and negative moment regions is less than 3.2% and 1.4%, respectively.

Table 10
Influence of stud diameter on plastic energy dissipation values

No.	η^+	space/mm	*d*/mm	plastic energy dissipation (kJ)					energy dissipation proportion of stud (%)	energy dissipation of each stud (J)
				concrete slab	steel girder	reinforcement	stud	total		
scb25	1.0	100	13	45.8	1259.5	132.8	5.0	1443.2	0.35	21.0
scb26	1.0	150	16	47.6	1276.2	136.8	5.3	1465.9	0.36	32.9
scb4	1.0	200	19	40.5	1274.7	127.3	3.9	1446.3	0.27	32.6
scb27	1.0	300	26	44.4	1264.2	116.1	4.6	1429.3	0.32	57.6
scb28	1.0	400	33	43.6	1264.7	126.3	4.7	1439.3	0.33	78.7

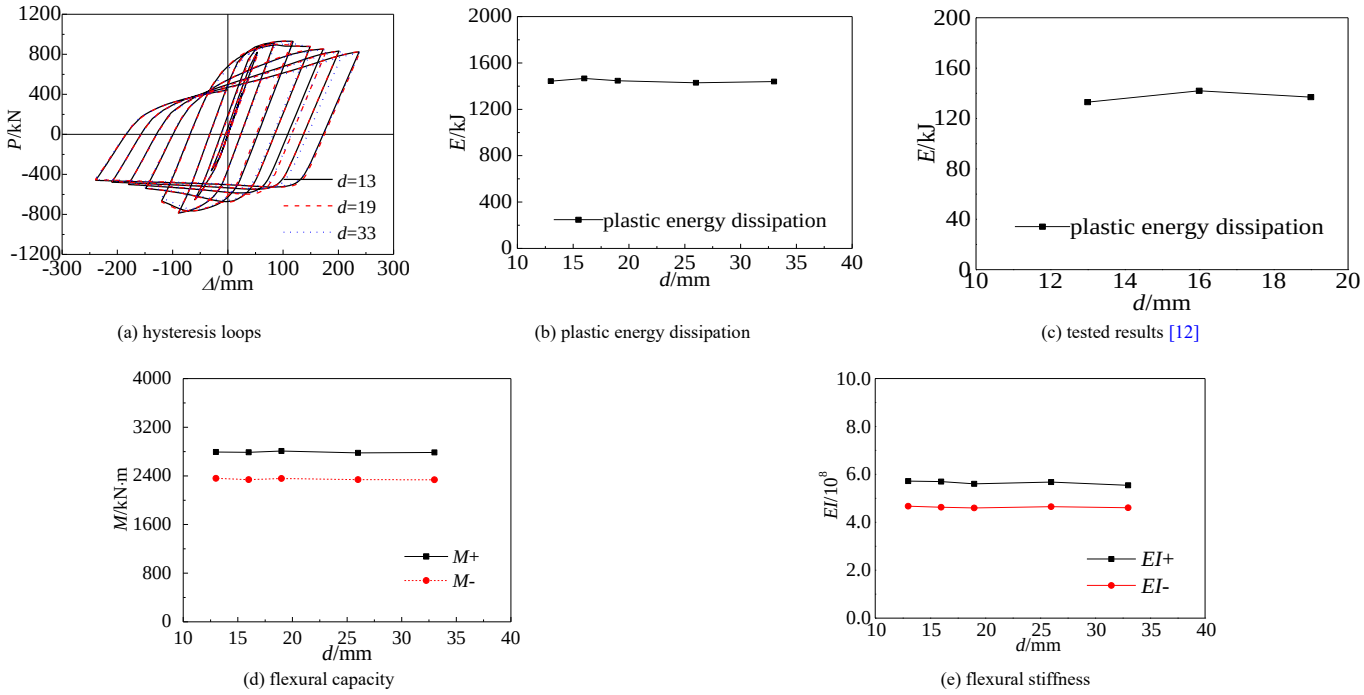

(a) hysteresis loops (b) plastic energy dissipation (c) tested results [12]

(d) flexural capacity (e) flexural stiffness

Fig. 19 Influence of stud diameter on the hysteresis performance of steel-concrete composite beams

4. Conclusions

The hysteresis behavior of steel–concrete composite beams were investigated by a validated 3D FE model using ABAQUS software. Based on the analysis, the following conclusions were drawn.

(1) A reasonable constitutive model of concrete and steel and an elaborate modelling method can be used to simulate the quasi-static behavior of steel-concrete composite beams accurately. In terms of load–displacement curve, load slip, and local buckling of steel beams, the calculated results are in good agreement with the measured values.

(2) The FEA results show that the steel girder is the main energy dissipation component of the composite beam, and the energy dissipation of the steel girder is higher than 80% of the total energy. The next is longitudinal reinforcement, followed by a concrete slab. The minimum proportion is the studs, and the energy dissipation of studs is less than 1% of the total energy. However, an increase in shear connection is beneficial to enhance the energy dissipation of steel beams and rebars.

(3) Shear connection, force ratio, and width–thickness ratio are the principal factors that influence the flexural capacity, flexural stiffness, and seismic performance of composite beams, respectively. That is, the higher the shear connection and force ratio are, the less the width–thickness ratio, the larger the capacity and stiffness, and the plumper the hysteretic curve will be. Transverse ratio, section form, and stud diameter slightly affect the seismic property of composite beams.

Acknowledgements

This research is financially supported by the National Natural Science Foundation of China under Grant Nos. 52008159, 51978664, and 52008400; Hunan Education Department Foundation Funded Project under Grant No. 21A0504; and China Postdoctoral Science Foundation under Grant No. 2018M632990.

References

[1] Ayoub A, Filippou FC. Mixed Formulation of Nonlinear Steel-Concrete Composite Beam Element. Journal of Structural Engineering. 2000;126:371-81.
[2] Bugeja MN, Bracci JM, Moore WP. Seismic behavior of composite RCS frame systems. Journal of Structural Engineering. 2000;126:429-36.
[3] Nie JG, Yu ZL, Ye QH. Seismic behaviour of composite steel-concrete beams. Journal of Tsinghua University (Science and Technology); 38(10):35-37. (in Chinese).
[4] Coughlan DJOG. The shear stiffness of stud shear connections in composite beams. Journal of Constructional Steel Research. 1986.
[5] Lam D, El-Lobody E. Behavior of Headed Stud Shear Connectors in Composite Beam. Journal of Structural Engineering. 2005;131:96-107.
[6] Ataei A, Zeynalian M, Yazdi Y. Cyclic behaviour of bolted shear connectors in steel-concrete composite beams. Engineering Structures. 2019;198:109455.1-.15.
[7] Xing Y, Han Q, Xu J, et al. Experimental and numerical study on static behavior of elastic concrete-steel composite beams. Journal of Constructional Steel Research. 2016;123:79-92.
[8] Chen J, Zhang H, Yu QQ. Static and fatigue behavior of steel-concrete composite beams with corroded studs. Journal of Constructional Steel Research. 2019;156:18-27.
[9] Jiang LZ, Yu ZW, Cao H, et al . Effect of shear connection degree on seismic resistant performance of steel-concrete composite beams. Journal of Building Structures, 38(3):52-54. (in Chinese)
[10] Nie J, Qin K, Cai CS. Seismic behavior of connections composed of CFSSTCs and steel–concrete composite beams—experimental study. Journal of Constructional Steel Research. 2007;64.
[11] Xue WC, Li K, Li J. Study on steel-concrete composite beams under low-reversed cyclic loading. Earthquake Engineering and Engineering Vibration, 22(6):65-70. (in Chinese)
[12] Ding FX, Liu J, Li XM, et al. Experimental investigation on hysteretic behavior of simply supported steel-concrete composite beam. Journal of Constructional Steel Research. 2018;144:153-65.
[13] Spacone E, El-Tawil S. Nonlinear Analysis of Steel-Concrete Composite Structures: State of the Art. Journal of Structural Engineering. 2004;130:159-68.
[14] Nie JG, Yu ZL, Yuan YS, et al. Research on restoring force model of composite steel-concrete beam. Journal of Tsinghua University (Science and Technology), 39(6),121-123.(in Chinese)
[15] Nie JG, Cai CS. Numerical modeling on concrete structures and steel–concrete composite frame structures. Composites Part B: Engineering. 2013.
[16] Tao MX, Nie JG. Fiber Beam-Column Model Considering Slab Spatial Composite Effect for Nonlinear Analysis of Composite Frame Systems. Journal of Structural Engineering. 2014;140:04013039.
[17] Zhao H, Kunnath SK, Yuan Y. Simplified nonlinear response simulation of composite steel–

concrete beams and CFST columns. Engineering Structures. 2010;32:2825-31.
[18] Nie J, Kai Q, Cai CS. Seismic behavior of connections composed of CFSSTCs and steel–concrete composite beams — finite element analysis. Journal of Constructional Steel Research. 2008;64:680-8.
[19] Bursi OS, Sun FF. Non-linear analysis of steel–concrete composite frames with full and partial shear connection subjected to seismic loads. Journal of Constructional Steel Research. 2005;61:67-92.
[20] Vasdravellis G, Valente M, Castiglioni CA. Behavior of exterior partial-strength composite beam-to-column connections: Experimental study and numerical simulations. Journal of Constructional Steel Research. 2009;65:23-35.
[21] Ding FX, Yin GA, Wang LP, et al. Seismic performance of a non-through-core concrete between concrete-filled steel tubular columns and reinforced concrete beams. Thin-Walled Structures. 2017;110:14-26.
[22] Liu J, Ding FX, Liu XM, et al. Study on flexural capacity of simply supported steel-concrete composite beam. Steel and Composite Structures. 2016;21:829-47.
[23] Ding FX, Ying XY, Zhou LC, et al. Unified calculation method and its application in determining the uniaxial mechanical properties of concrete. Frontiers of Architecture & Civil Engineering in China. 2011;5:381.
[24] Simulia. (2014), Abaqus/standard user's manual, version 6.14 edition, Providence, RI: Dassault Systemes.
[25] Yao X-m, Zhou XH, Guan Y, Shi Y, He Z-q. 'Bending behavior of cold-formed steel–concrete composite floors.' Advanced Steel Construction. 2019;15(4).
[26] Bahaz A, Amara S, Jaspart J-P, Demonceau J-Fo. 'Numerical analysis and evaluation of effective slab width of composite continuous beams with semi-rigid joint.' Advanced Steel Construction. 2021;17(4):9.
[27] Zou Y, Zhou XH, Di J, Qin FJ. 'Partial interaction shear flow forces in simply supported composite steel-concrete beams.' Advanced Steel Construction. 2018;14(4):17.
[28] Yao X-m, Zhou XH, Guan Y, Shi Y, He Z-q. 'Bending behavior of cold-formed steel–concrete composite floors.' Advanced Steel Construction. 2019;15(4).
[29] Pardeshi RT, Patil YD. Review of various shear connectors in composite structures. Advanced Steel Construction. 2021;17(4):9.
[30] GB 50017-2017 (2017), Standard for design of steel structure; Architecture and Building Press, Beijing, China
[31] Ding FX, Ni M, Gong YZ, et al. Experimental study on slip behavior and calculation of shear bearing capacity for shear stud connectors. Journal of Building Structures, 35(9):98-106. (in Chinese)